ORNL/SPR-2022/2641

Impact of annealing at 1000°C in flowing He with low O_2 concentration on the room temperature tensile properties of Mo alloys

Sebastien Dryepondt
Adam Willoughby
Brandon Johnston

September 2022

OAK RIDGE National Laboratory

ORNL IS MANAGED BY UT-BATTELLE LLC FOR THE US DEPARTMENT OF ENERGY

DOCUMENT AVAILABILITY

Reports produced after January 1, 1996, are generally available free via OSTI.GOV.

Website www.osti.gov

Reports produced before January 1, 1996, may be purchased by members of the public from the following source:

National Technical Information Service
5285 Port Royal Road
Springfield, VA 22161
Telephone 703-605-6000 (1-800-553-6847)
TDD 703-487-4639
Fax 703-605-6900
E-mail info@ntis.gov
Website http://classic.ntis.gov/

Reports are available to US Department of Energy (DOE) employees, DOE contractors, Energy Technology Data Exchange representatives, and International Nuclear Information System representatives from the following source:

Office of Scientific and Technical Information
PO Box 62
Oak Ridge, TN 37831
Telephone 865-576-8401
Fax 865-576-5728
E-mail reports@osti.gov
Website https://www.osti.gov/

This report was prepared as an account of work sponsored by an agency of the United States Government. Neither the United States Government nor any agency thereof, nor any of their employees, makes any warranty, express or implied, or assumes any legal liability or responsibility for the accuracy, completeness, or usefulness of any information, apparatus, product, or process disclosed, or represents that its use would not infringe privately owned rights. Reference herein to any specific commercial product, process, or service by trade name, trademark, manufacturer, or otherwise, does not necessarily constitute or imply its endorsement, recommendation, or favoring by the United States Government or any agency thereof. The views and opinions of authors expressed herein do not necessarily state or reflect those of the United States Government or any agency thereof.

ORNL/SPR-2022/

Materials Science and Technology Division

IMPACT OF ANNEALING AT 1000°C IN FLOWING HE WITH LOW O_2 CONCENTRATION ON THE ROOM TEMPERATURE TENSILE PROPERTIES OF MO ALLOYS

Author(s)

Sebastien Dryepondt
Adam Willoughby
Brandon Johnston

September 2022

Prepared by
OAK RIDGE NATIONAL LABORATORY
Oak Ridge, TN 37831
managed by
UT-BATTELLE LLC
for the
US DEPARTMENT OF ENERGY
under contract DE-AC05-00OR22725

CONTENTS

ABSTRACT

NorthStar is developing an accelerator-based technology to produce the medical isotope Mo-99. A previous ORNL report (ORNL/SPR-2022/2490) studied the oxidation behavior of Mo in flowing He with low oxygen content at 800°C and 1000°C and it was shown that an O_2 concentration lower than ~5ppm (µl/l) is required to achieve acceptable oxidation rates for wrought or powder metallurgy (PM) Mo. Oxidation may also impact the mechanical properties of Mo and this report summarizes tensile results at room temperature on wrought and PM Mo before and after exposure at 1000°C in flowing He with O_2 concentration varying from 1 to 15 ppm O_2. It was found that oxidation at 1000 °C results in a significant decrease of Mo strength and ductility with brittle intergranular fracture surfaces, likely due to the segregation of oxygen at grain boundaries. For the PM Mo material, the decrease in strength and ductility was also observed after annealing in vacuum at 1000 °C, indicating that the diffusion of the oxygen trapped in the material pores to grain boundaries after 20-100 h at 1000 °C is sufficient to embrittle the material. Finally, initial results on actual aMo and high-density disks provided by NorthStar revealed the lack of ductility of the materials due to the specific disk microstructure.

1. INTRODUCTION

Molybdenum-99 is a key isotope for a broad range of diagnostic procedures, but the isotope supply depends on foreign countries and current production method requires nuclear reactors. The NNSA's Mo-99 program is focused on the domestic production of Mo-99 using methods that do not require highly enriched uranium, such as NorthStar's electron-beam accelerator. In the accelerator, thin Mo-100 targets ~1inch in diameter will be exposed for a week to a high energy electron beam to produce Mo-99. The targets will be cooled by a Helium gas flowing at a rate superior to 50m/s but the targets will still be exposed to temperatures ranging from ~200 °C at the edges to 1000 °C in the center[1]. A previous report focused on the impact of low O_2 concentration in the He gas at 800 °C and 1000 °C on the oxidation behavior of both sheet and powder metallurgy Mo[2]. It was found that concentration as low as 15 ppm O_2 in an He gas flowing at 1 m/s can result in significant mass losses after 20 to 100 h at 1000 °C due to the growth and volatilization of an Mo oxide scale. Significant redeposition of the volatilized Mo oxide was also observed in colder areas of the furnace, which could also be a significant concern for the accelerator. Decreasing the oxygen concentration to less than 5 ppm by using high purity He drastically reduced the oxidation kinetics and resulted in either very low mass losses or mass gains.

Another potential issue to be addressed is the Mo target embrittlement due to high temperature oxidation. Liu et al.[3] conducted oxidation testing on 0.51 mm thick Mo sheet at 1150 °C in low pressure oxygen (1.3 mPa) for durations ranging from 100 h to 612 h and they observed a significant increase of the Mo sheet ductile to brittle transition temperature (DBTT), from slightly below room temperature[4,5] to ~200 °C. Contrary to many other refractory alloys such as Ta, Zr or Nb, the oxygen solubility in Mo is very low, less than 1 ppm[6], but segregation of oxygen at grain boundary can lead to significant grain boundary embrittlement [3]. Carbon is also known to segregate at grain boundaries and might hinder the effect of oxygen[7,8]. Even for Mo material with very low level of impurities, several researchers have demonstrated the intrinsic nature of some Mo grain boundaries depending on the grains misorientation angle [9,10]. To assess Mo target embrittlement, small scale dog bone tensile specimens made of sheet and powder metallurgy Mo alloys were exposed in vacuum and flowing He with O_2 concentration varying from 0.5 to 5 ppm O_2 for 5 h to 100 h.

2. EXPERIMENTAL PROCEDURE

2.1 Materials

Most of the tests were conducted on either a wrought Mo sheet, 0.5 mm thick, or powder metallurgy (PM) thin plates, 0.8 mm thick. The wrought Mo sheet with 99.9% purity was purchased from Goodfellow in the annealed stress-relieved condition. The microstructure of the sheet material is shown in Figure 1a. Small grains were observed, ~1μm in size, with slightly elongated grains along the rolling direction and a very limited number of very small defects. One inch dog-bone type specimens similar to the one shown in Figure 1c were machined parallel and perpendicular to the rolling direction.

The PM Mo plates, fabricated from H. C. Starck spray-dried molybdenum powder with 99.9% purity, were sintered at 1600 °C for 4 h with an applied stress of 775 MPa and with the addition of 0.5 wt% of ethylenebisstearimide (EBS) as lubricant. The dimensions of the sintered plates were approximately 44 mmx 24.6 mm x 0.8mm and the measured density was 87 to 89 % compared to the theoretical density value. The resulting microstructure is presented in Figure 1b and 1g showing ~20μm equiaxed grains and the presence of voids, ~0.5 to 5μm in size (black arrows), in the grain and at grain boundaries. Small SS3-type dog bone specimens were machined along the plates width and examples are given in the as fabricated condition (Fig. 1d), or after annealing for 20 h at 1000 °C in vacuum (Fig. 1e) or flowing UHP He (Fig. 1f) . The SS3 specimens were slightly smaller compared to the specimens machined from the Mo sheet to maximize the number of specimens per plate.

SS3 tensile specimens were also machined from high density (HD) and enriched aMo disks provided by Northstar. Figure 2 shows that three specimens were machined per disk with two of the specimens exhibiting rounded corners in the specimen head, which was not considered as an issue since the specimens are shoulder-loaded during tensile testing. One aMo tensile specimen cracked during machining in one of the specimen heads but the specimen failed in the gage section during tensile testing. For the HD disk, machining was performed using either electro discharge machining (EDM) or water jetting (WJ) to assess the potential impact of machining process on the HD Mo tensile properties. For all the EDM specimens, the gage section width was repolished to remove the EDM affected zone. All the tensile specimens were cleaned in ethanol and methanol prior to testing and dimensions were measured using both a Keyence 3D microscope and a caliper.

Finally, cross-section optical micrographs of the Mo disks are shown in Figure 4. A quite high density of pores homogeneously distributed, ~5μm in size, was observed for the aMo disk. On the contrary, the distribution of voids was quite inhomogeneous in the HD disks with the presence of larger defects, ~20μm in size.

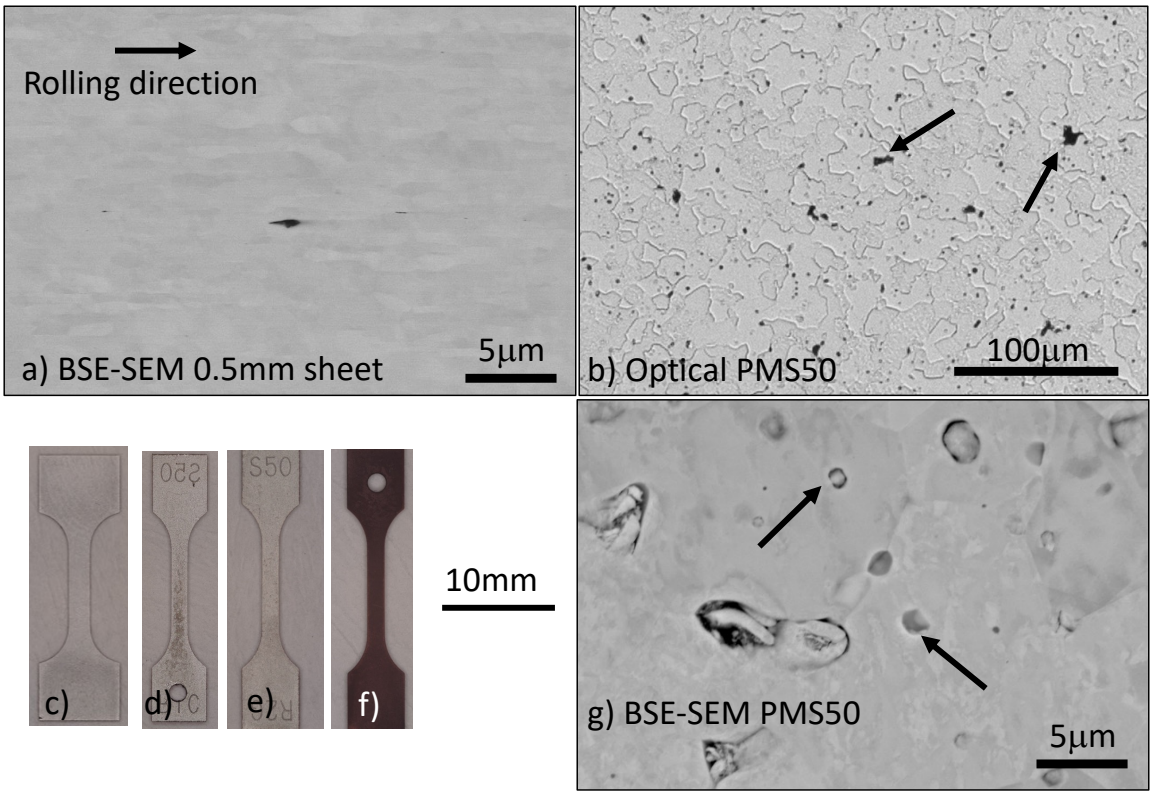

Figure 1: a) BSE-SEM micrographs showing the grain structure of the 0.5 mm sheet, b) and g) Optical and BSE-SEM micrographs showing the microstructure of the PMS50 Mo material, c) optical top view image dog bone tensile specimens, d)-f) Optical top-view image SS3-type specimens, d) as machined, e) after 20 h at 1000 °C in vacuum, f) after 20 h at 1000 °C in flowing UHP He

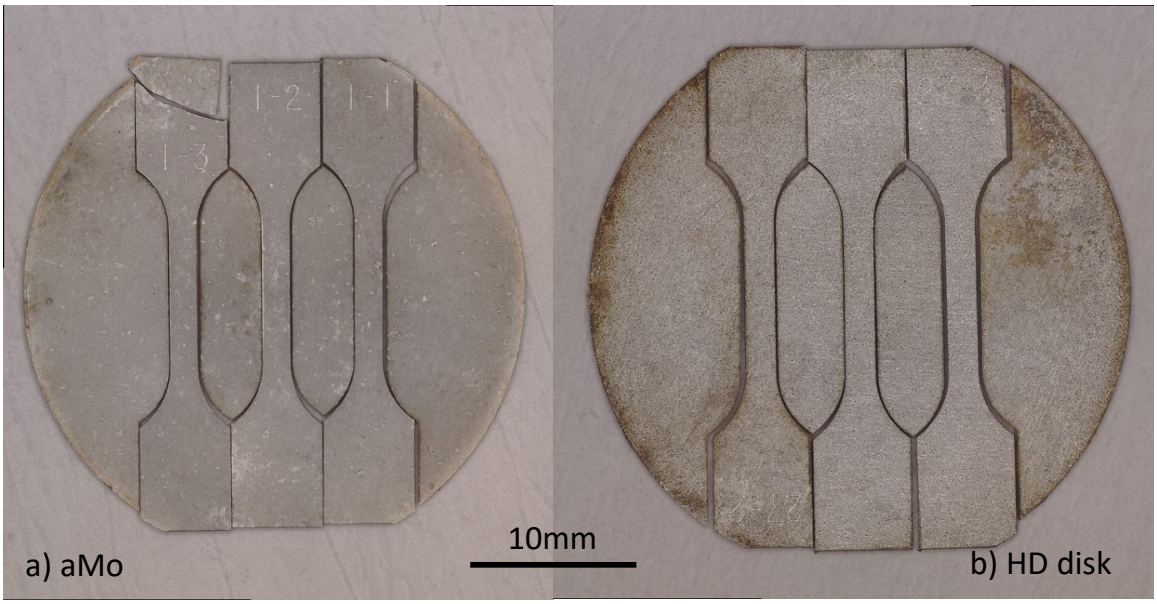

Figure 2: Top view optical images of SS3 tensile specimens machined from a) an aMo disk, b) a HD Mo disk

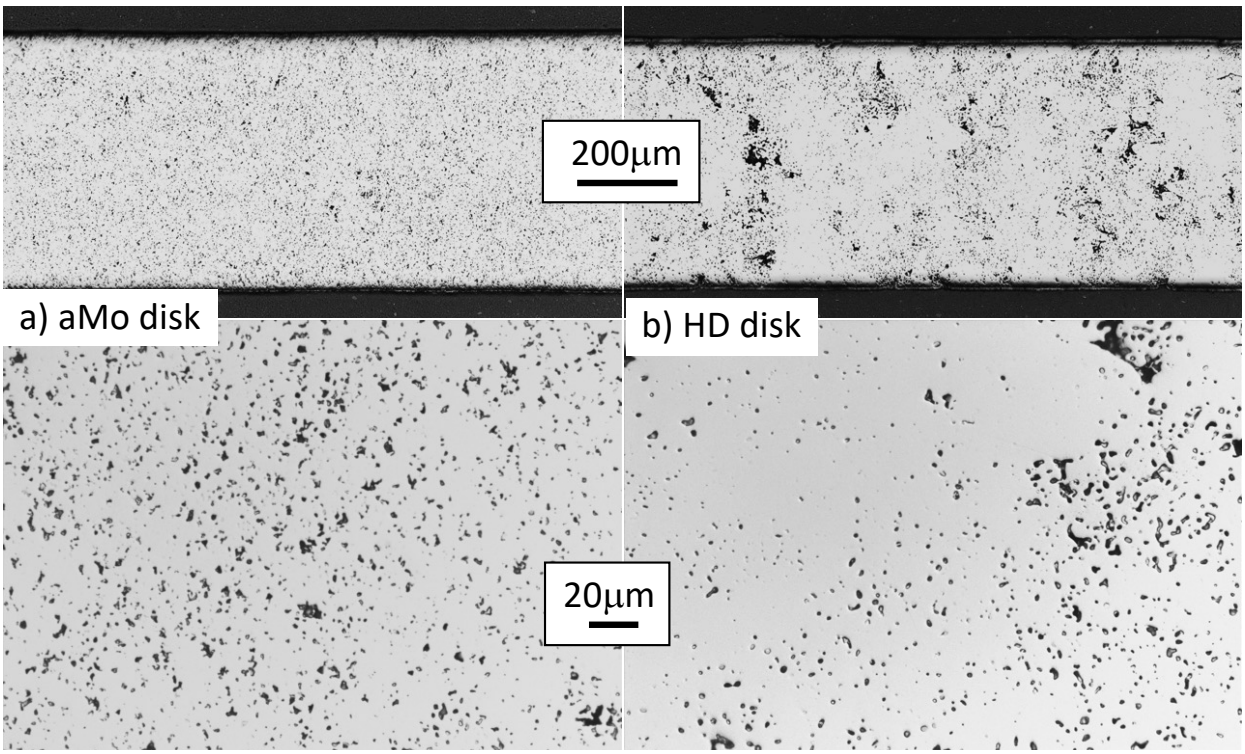

Figure 3: Cross-section optical micrographs of as received material, a) aMo disk, b) HD Mo disk

2.2 Oxidation testing

As can be seen in Figure 4, oxidation testing was conducted at 1000 °C in a quartz tube inserted in a calibrated three-zone furnace. Glass to metal seals were welded to the quartz tube and vacuum grade copper seals (Fig. 3c) were used to avoid oxygen ingress and control the oxygen content at very low ppm levels. GE oxy.IQ oxygen sensors were used to measure the oxygen concentration at the inlet and outlet of the oxidation rigs. An alumina tube with a 6.3mm internal diameter was inserted in the quartz tube and connected to the gas inlet to reach a gas velocity of ~1m/s with a flow rate 500 cm^3 /min (Fig. 3b). A thin slot in the alumina tube allowed insertion of a dog bone specimen. For the smaller SS3 specimen, a 1 mm hole was machined in one of the head of the specimen and in the alumina tube allowing the use a thin Pt wire to pin the specimen. The oxygen content in the He gas was controlled using high purity (HP) and ultra-high purity (UHP) He cylinders with maximum O_2 concentration of 5 ppm and 1 ppm, respectively. Pre-mixed He certified gases were also purchased with 1 ppm, 5 ppm or 15 ppm O_2. An identical oxidation rig was slightly modified to conduct exposure in vacuum using a rougher pump with a vacuum of ~10^{-3} torr. Further details on the development of the oxidation rigs can be found on the report focused on the oxidation behavior of the Mo alloys.

2.3 Tensile Testing

Tensile testing was carried out at room temperature using an Instron electro-mechanical machine. Extensometers could not be attached to the SS3-type specimens, so the specimen deformation was estimated using the crosshead displacement with a displacement rate corresponding to a strain rate of ~10^{-3} s^{-1}. A pre-

load of ~20 lbs was typically used to align the specimens with the load train which resulted in the failure of a few oxidized specimens before testing as will be discussed later.

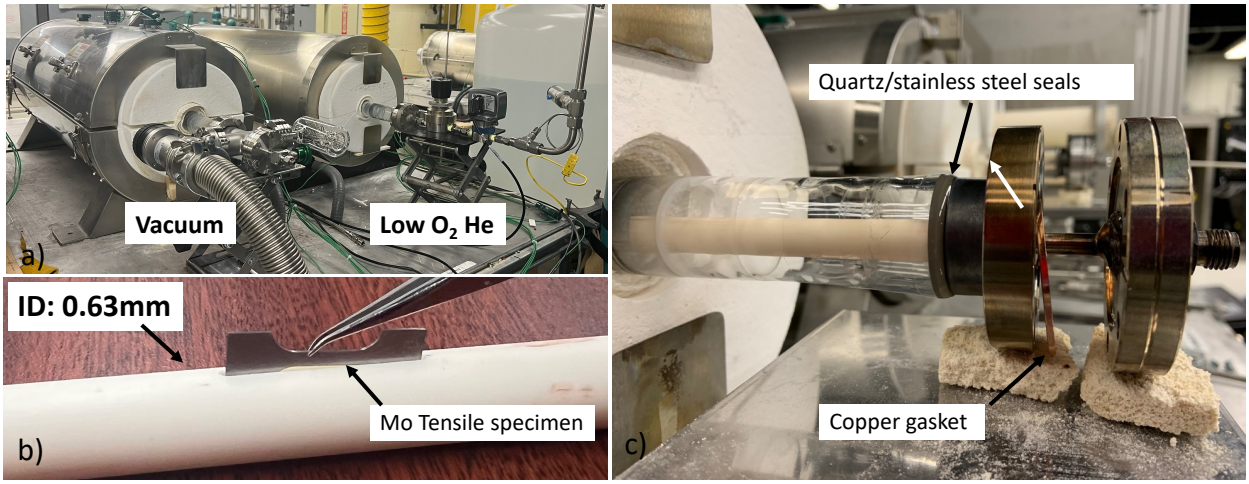

Figure 4: a) Oxidation testing rig, vacuum and flowing He with 1 to 15 ppm O_2, alumina tube inserted in the quartz tube to accelerate He gas velocity, c) Glass to metal seals welded to the quartz tube and vacuum grade copper gasket

2.4 Specimen characterization

As fabricated materials were cut using a low-speed saw, mounted in epoxy, and polished using colloidal silica for the final polishing step. Optical and scanning electron microscopy (SEM) images were acquired using a Zeiss optical light microscope and a Tescan Mira3 SEM, respectively. Fracture surface analysis of the specimens after tensile testing was conducted using an Hitachi 4800 SEM equipped with an energy dispersive X-ray spectroscopy (EDS) detector for chemical analysis.

3. RESULTS AND DISCUSSION

3.1 Wrought Mo sheet

Table 1 and Figure 5 summarize all the tensile tests conducted at room temperature on the 0.5 mm Mo sheet in the as fabricated condition and after exposure at 1000 °C in various atmospheres. As can be seen in Figure 4a, the strain is overestimated in the elastic portion of the tensile curves due to the compliance of the tensile machine. For this reason, strain or ductility at rupture in this report refers to the total plastic deformation. It is worth noting that for all the specimens no uniform elongation was observed, with most of the strain being therefore related to specimen necking. The yield strain and ultimate tensile strength (UTS) are, therefore, quite similar. For the as fabricated specimens, testing along the rolling direction resulted in slightly higher ductility and lower yield strength compared to specimens tested perpendicular to the rolling direction (Fig. 4b and 4c). This difference is likely due to the grain structure elongated along the rolling direction (Fig. 1a).

Specimens annealed in vacuum exhibited significant increase in ductility and decreases in yield strength and UTS compared to the as fabricated 0.5 mm Mo sheet. Such changes in tensile properties are likely related to the (partial) recrystallization of the sheet during annealing at 1000 °C for 100 h. The specimens

were not cross-sectioned, but Figure 6 shows, for example, large grains in the center of specimens annealed for 20 h at 1000 °C in flowing He with 15 ppm O_2 or 100 h at 1000 °C in UHP He. Yu and Kumar [6] conducted tensile testing on 1.5 mm Mo sheet before and after recrystallization at 1300 °C for 2 h, and they also observed a significant increase in ductility and decrease in strength due to the recrystallization annealing step. Recrystallization of Mo is often considered as detrimental due to a decrease of both strength and ductility[10]. While the lower strength for large-grain recrystallized Mo is directly related to the well-known Hall Petch effect, decrease in ductility has been attributed to segregation of oxygen at grain boundaries due to the high temperature recrystallization heat treatment. Cockeram et al. demonstrated, however, that a recrystallization step at 1300°C or 1400°C could increase the ductility of high purity low oxygen low carbon arc cast molybdenum[11].

Annealing in flowing He with O_2 concentration varying from ~1 ppm O_2 to 15 ppm O_2 also resulted in a decrease of the foil strength, but not as pronounced as the one observed in vacuum. In addition, a significant decrease in ductility was observed for all the exposed foils, with plastic strain at rupture ranging from 0 to 6 % compared to ~12 % for the as fabricated material. The specimens tested for 20 h, either in UHP He or He with 15ppm O_2, showed higher ductility than the two specimens tested for 100 h in UHP indicating that duration of exposure had more of an impact than the O_2 content in the He gas. All these results are consistent with Liu et al.[2] results on Mo tensile specimens oxidized in low PO_2 atmosphere at 1150 °C, with a ductility decreasing from ~50% before exposure down to nearly 0 after 100 h in 1.3 mPa O_2.

Figure 7 shows BSE-SEM micrographs of the fracture surface of several of these wrought tensile specimens. The recrystallization after vacuum annealing drastically changed the fracture surfaces between the as machined and recrystallized specimens. While a ligament-like structure was observed for the as fabricated specimens[5,11], the specimen annealed in vacuum exhibited a ductile fracture. In both cases, the specimen deformation was mainly related to specimen necking with a significant surface area reduction. On the contrary, limited necking was observed for the specimens annealed in flowing He with 15 ppm of O_2 or UHP He, with clear evidence of brittle intergranular fracture. It is worth noting that the center of the fracture specimen exhibited large, recrystallized grains while smaller grains appeared to be present at the specimen edges, as observed in the cross-section micrographs in Figure 6.

Table 1: Summary of the oxidation data and tensile properties for the 0.5 mm wrought Mo sheet before and after annealing at 1000 °C.

Conditions	Yield Strength (MPa)	UTS (MPa)	Strain (%)	In O_2 (ppm)	Out O_2 (ppm)	Mass change mg/cm^2
As Polished RD	675.8	703.5	9.22	NA	NA	NA
As Polished RD	680.2	703.2	12.2	NA	NA	NA
As machined RD	665.4	696.1	9.6	NA	NA	NA
As machined RD	696.3	743.9	17.7	NA	NA	NA
As machined RD	697.7	747.5	15	NA	NA	NA
As machined Per. RD	727.8	744.3	9.9	NA	NA	NA
As machined Per. RD	693.2	713.1	10.1	NA	NA	NA
As machined Per. RD	698.6	715.5	10.9	NA	NA	NA
20h in vaccum RD	482.2	490.4	26.5	NA	NA	0.14
20h in vacuum Per. RD	503.4	520.4	18.2	NA	NA	0.15
20h UHP He RD	582.4	585.7	2.97	0	2	0.29
100h UHP He RD	555	557	0.6	0.5	1.5	-0.89
100h UHP He RD	542.7	543.9	0.66	0	8	-1.26
20h 15ppmO2 RD	593.2	597.6	5.3	9	15	-2.77

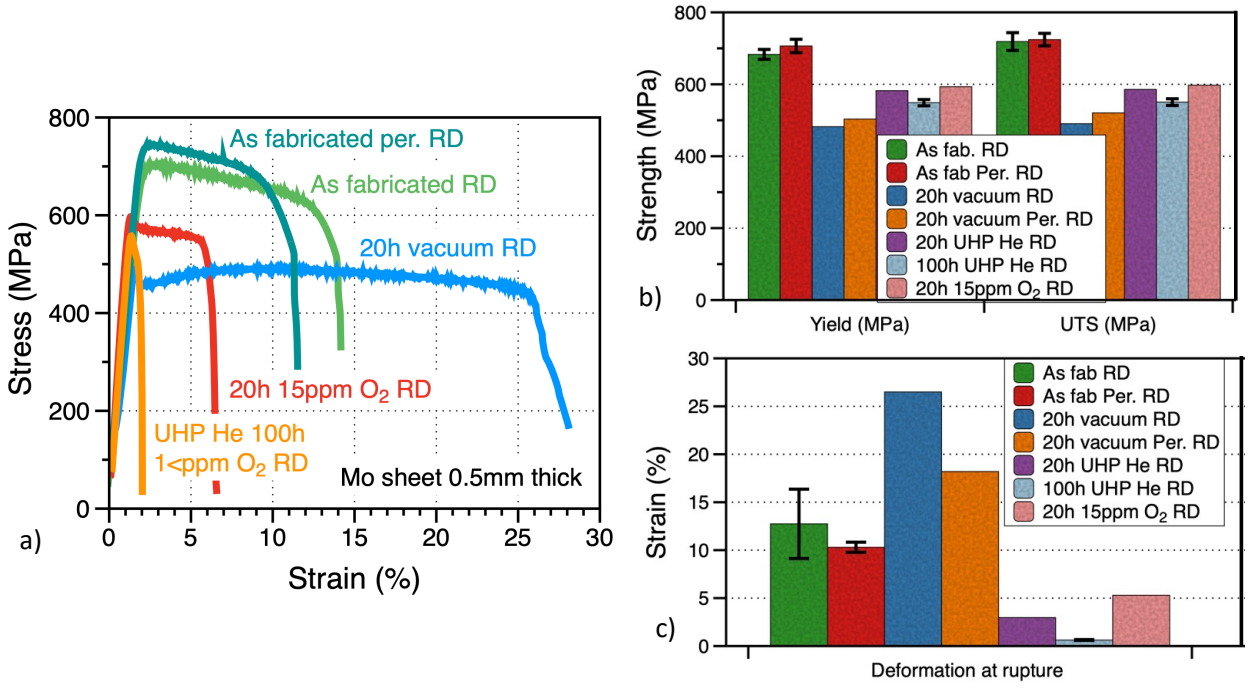

Figure 5: Tensile results at room temperature for the 0.5 mm Mo wrought sheet before and after annealing at 1000 °C, a) examples of tensile curves, b) Yield and UTS, c) Plastic deformation at rupture

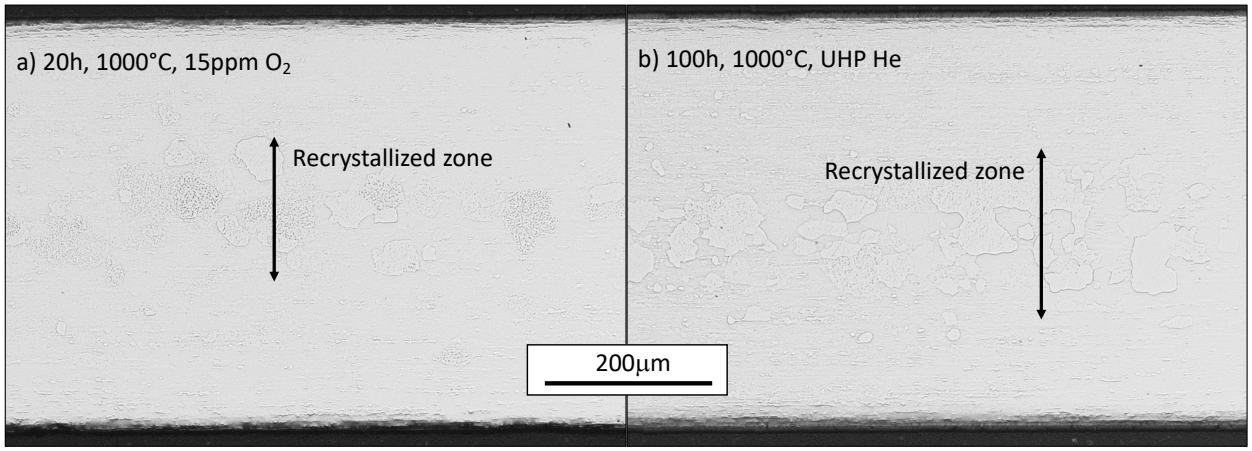

Figure 6: Optical cross-section micrographs of the 0.5 mm wrought Mo sheet after exposure, a) for 20 h at 1000 °C in flowing He with 15 ppm O_2 and b) for 100 h at 1000 °C in UHP He .

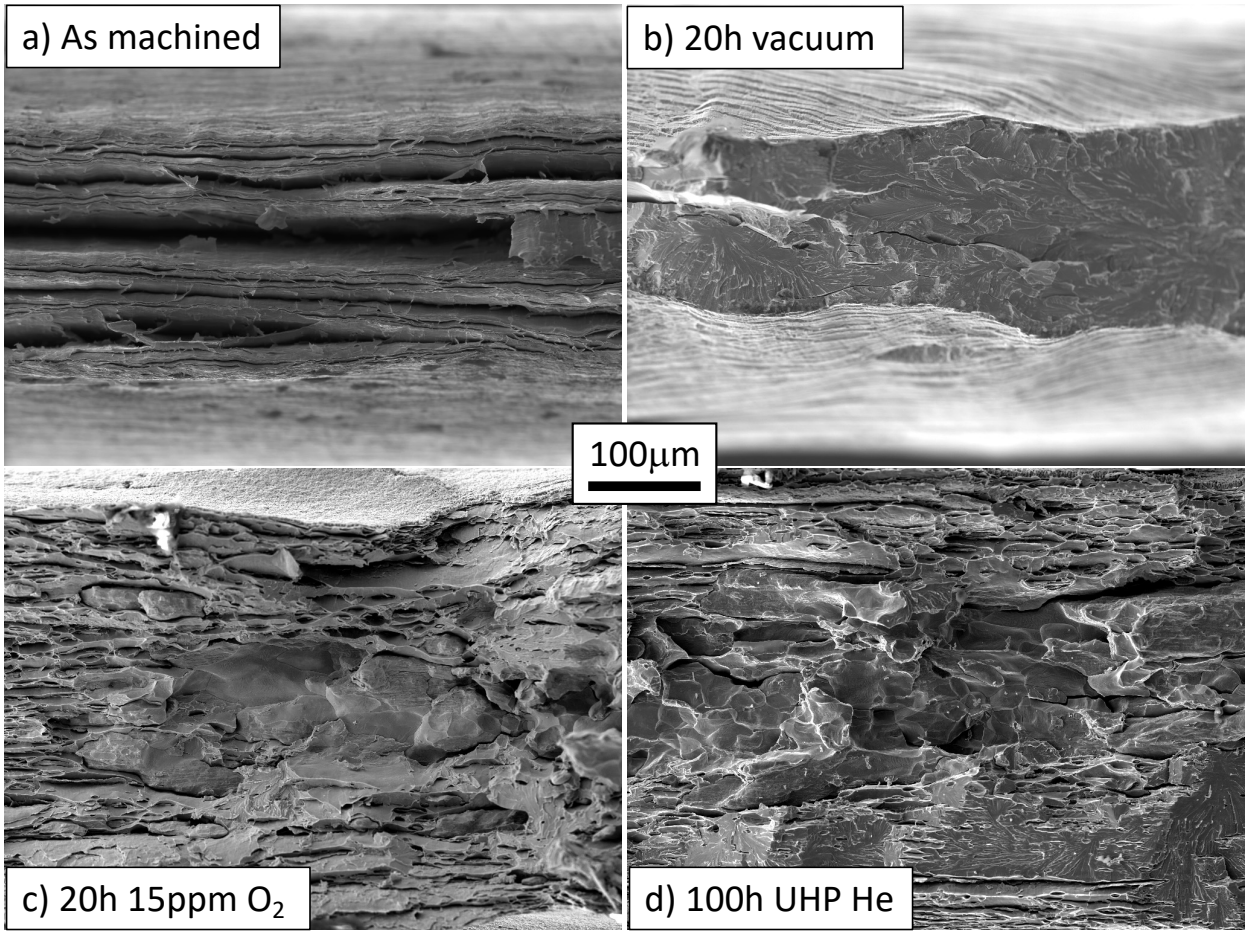

Figure 7: BSE-SEM images of the fracture surface after tensile testing at room temperature of 0.5 mm wrought Mo specimens annealed at 1000 °C, a) As machined specimen, b) 20 h in vacuum, c) 20 h in flowing He with 15 ppm O_2, d) 100 h in flowing UHP He.

3.2 PMS50 Mo sheet

A summary of the room temperature tensile properties for the PMS50 material before and after exposure at 1000 °C in vacuum or flowing He gases with low O_2 content are presented in Table 2 and Figure 8. One tensile test was conducted in the as machined condition and Figure 8b and 8c shows that the yield strength, UTS and plastic strain measured were consistent with previous data generated using 6 specimens. Arrows in Figure 8a highlight the occurrence of sudden decreases and increases of stress during tensile testing of the as machined specimen. This is likely due to the presence of voids (Figure 1b and 1c) and sudden propagation of small cracks in the ~88% dense material. Exposure at 1000 °C in vacuum or flowing He with low O_2 content resulted in a drastic decrease in ductility, to such an extent that several specimens annealed in UHP He, broke during specimen preparation before testing. Large variations in yield strength and UTS were observed due to the sudden rupture of the specimen while still in the elastic portion of the tensile curve (Figure 8a).

Table 2: Summary of the oxidation data and tensile properties for the PMS50 Mo plates before and after annealing at 1000 °C.

Conditions	Yield Strength (MPa)	UTS (MPa)	Strain (%)	In O_2 (ppm)	Out O_2 (ppm)	Mass change mg/cm^2
As machined	368	396.7	12	NA	NA	NA
100h UHP He	broke before testing			0 ppm	0 ppm	-0.44
20h UHP He	broke before testing			0 ppm	0 ppm	0.1
UHP 20h	broke before testing					0.15
1ppm 100h	202.9	202.9	0	0.3	0	0.1
5ppm 20h	135.9	135.9	0	3.2	4.9	
Vaccum 20h	322	322	2.5	NA	NA	
Vaccum 5h	209.5	209.5	0	NA	NA	0
High Vaccum 100h	276	300.9	2	NA	NA	-0.28

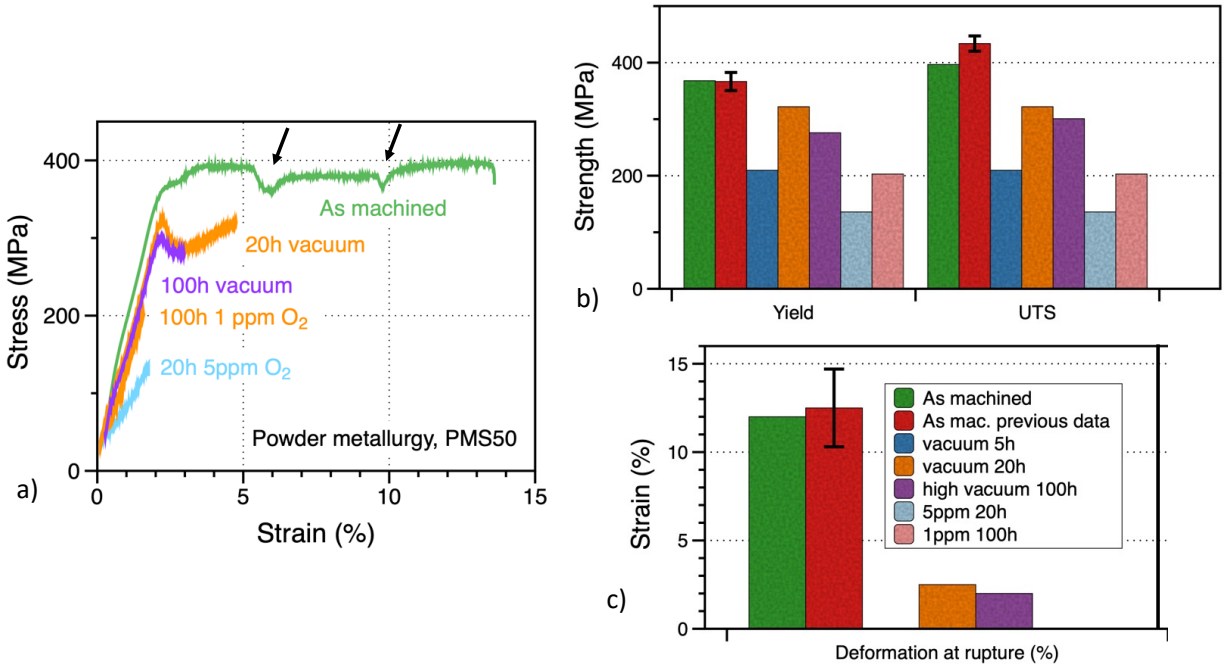

Figure 8: Tensile results at room temperature for the PMS50 thin Mo plates before and after annealing at 1000 °C, a) examples of tensile curves, b) Yield strength and UTS, c) Plastic deformation at rupture

Examples of fracture surfaces are presented in Figure 9 and Figure 10. Moderate ductility was observed for the as machined specimen with what appears to be a mix of transgranular and intergranular fracture surface (Fig. 10a). For all the specimens annealed at 1000 °C, a brittle transgranular fracture surface was clearly observed (Fig. 10b-10d). The higher magnification BSE-SEM micrographs in Figure 11 highlight the presence of small precipitates at the fracture surface for all the specimens except for the as machined specimen. As shown in Figure 12, EDS analysis revealed that these precipitates were likely Mo-rich oxides. It is worth noting that these precipitates were also observed for the specimens annealed in vacuum, suggesting that oxygen was already present in the specimen, likely trapped in voids, migrated at grains boundaries after high temperature annealing to form these precipitates. As observed here, Liu et al.[2] proposed that segregation of oxygen at grain boundaries after exposure in 1.3 mPa PO_2 at 1150 °C was the reason for drastic embrittlement of Mo at high temperature.

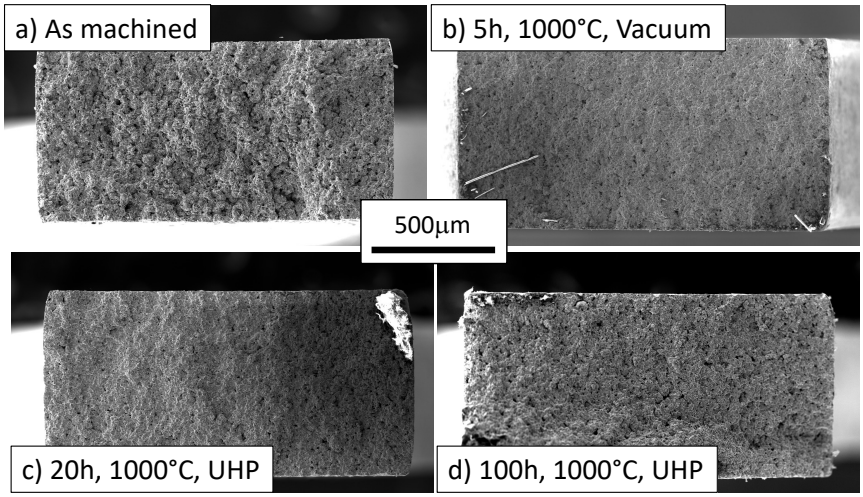

Figure 9: BSE-SEM images of the fracture surface after tensile testing of PMS50 Mo specimens annealed at 1000 °C, a) As machined specimen, b) 5 h in vacuum, c) 20 h in flowing UHP He, d) 100 h in flowing UHP He.

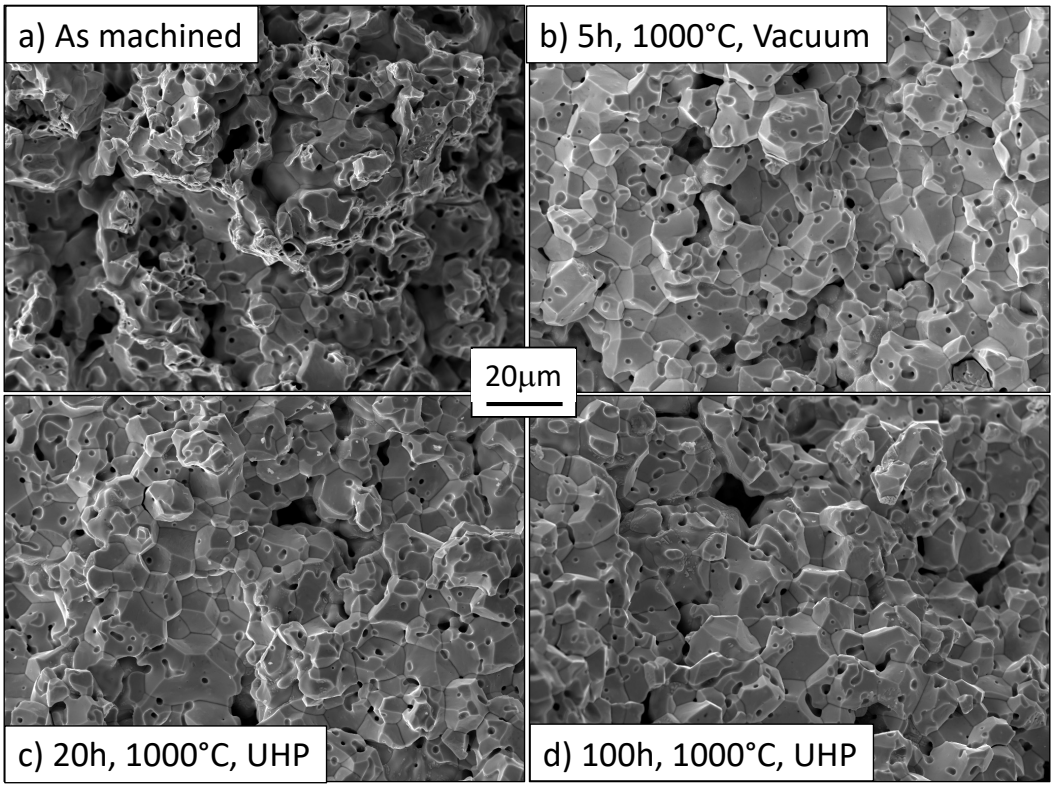

Figure 10: BSE-SEM images of the fracture surface of PMS50 Mo specimens annealed at 1000 °C, a) As machined specimen, b) 5 h in vacuum, c) 20 h in flowing UHP He, d) 100 h in flowing UHP He

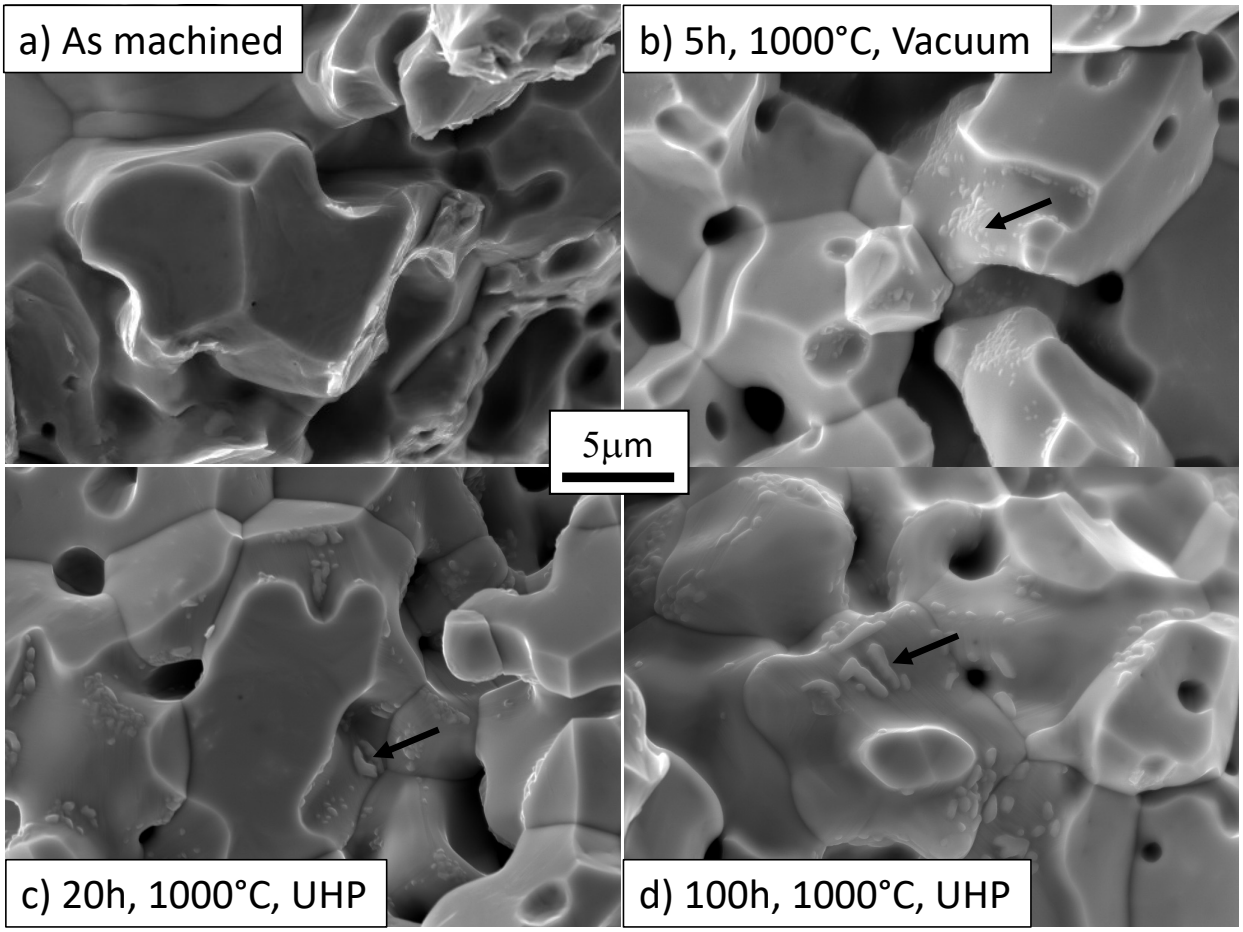

Figure 11: BSE-SEM images of the fracture surface after tensile testing at room temperature of PMS50 Mo specimens annealed at 1000 °C, a) As machined specimen, b) 5 h in vacuum, c) 20 h in flowing UHP He, d) 100 h in flowing UHP He.

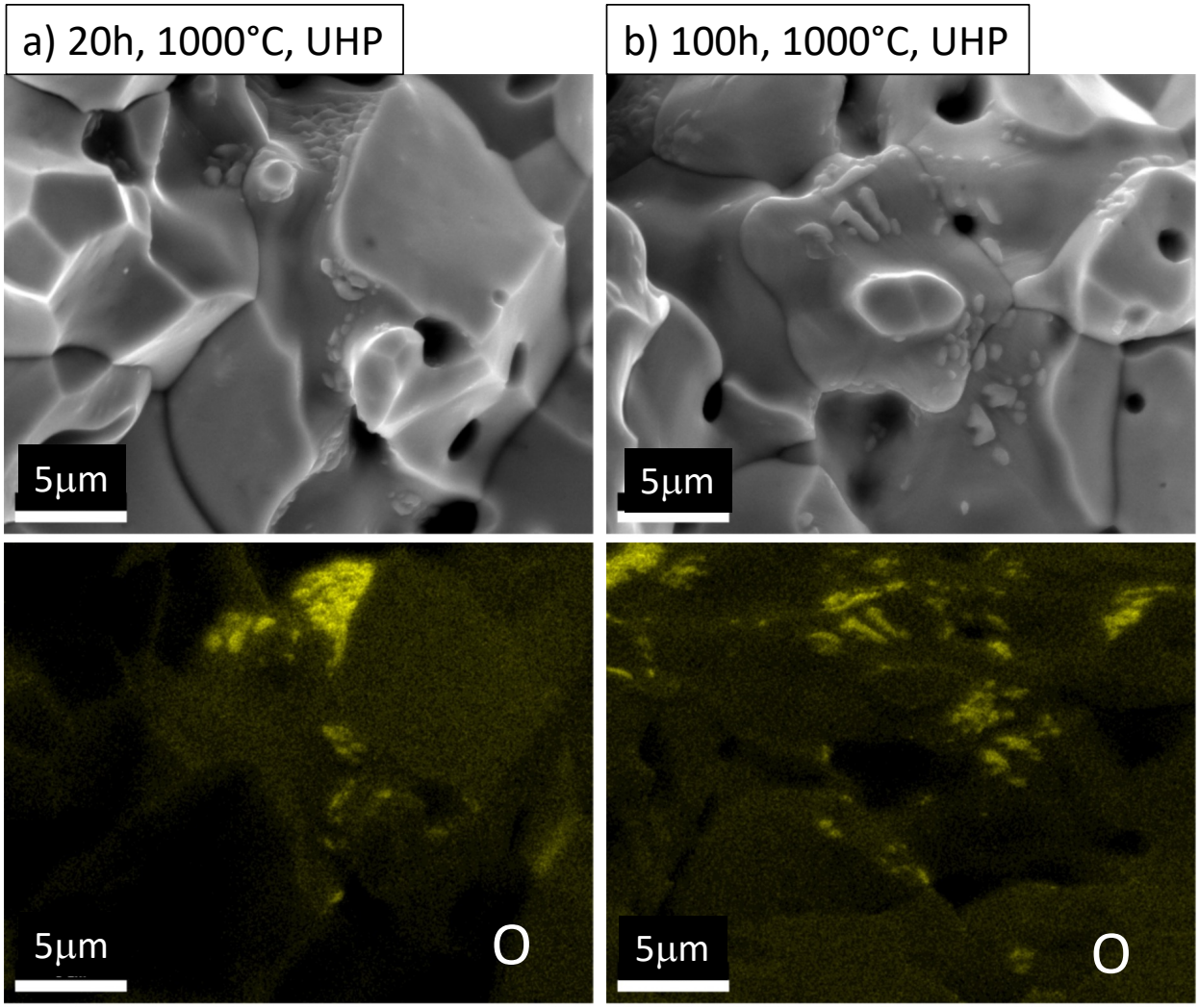

Figure 12: BSE-SEM micrographs and corresponding oxygen EDS maps of the fracture surfaces of specimens annealed at 1000 °C in flowing UHP He, a) 20 h, b) 100 h.

3.3 Mo disks

As shown in Figure 2, tensile specimens were machined from Mo disks provided by Northstar and the resulting room temperature tensile properties are compared in Figure 13 with the tensile properties for the wrought Mo sheet and the PMS50 Mo material. The aMo material exhibited tensile strength superior to the strength of the PMS50 material but with very low ductility ie. ~1% plastic strain at rupture. Further embrittlement was observed after annealing for 100 h at 1000 °C in flowing UHP He, leading to no ductility and yield strength and UTS down to ~150Mpa. Lower strength was measured for the as fabricated HD disks but slightly better average ductility with significant variation from one specimen to another. One specimen machined by EDM exhibited a ductility of 5 %, while the two other disks, one machined by EDM and the other one machined by water jetting (WJ) failed after 1 % plastic deformation.

Figure 14 compares the fracture surface of the as fabricated aMo and HD specimens. In both cases, a brittle intergranular fracture was observed, but with very different grain structures. For the aMo material,

small grains ~1μm in size were homogeneously distributed, while a more heterogenous grain structure was observed for the HD disks, as seen in Figure 3, with regions of small grains, less than 10 μm in size and regions of larger grains, >20μm in size.

The fracture surface of the aMo specimen annealed for 100 h at 1000 °C in flowing HP He looked similar to the fracture of the as-fabricated specimen, but the high magnification BSE-SEM micrographs shown in Figure 15 highlight the presence of very small precipitates, as observed previously for the annealed PMS50 specimens. EDS mapping revealed again that these precipitates were Mo oxides, confirming segregation of oxygen at grain boundaries as a key embrittlement mechanism.

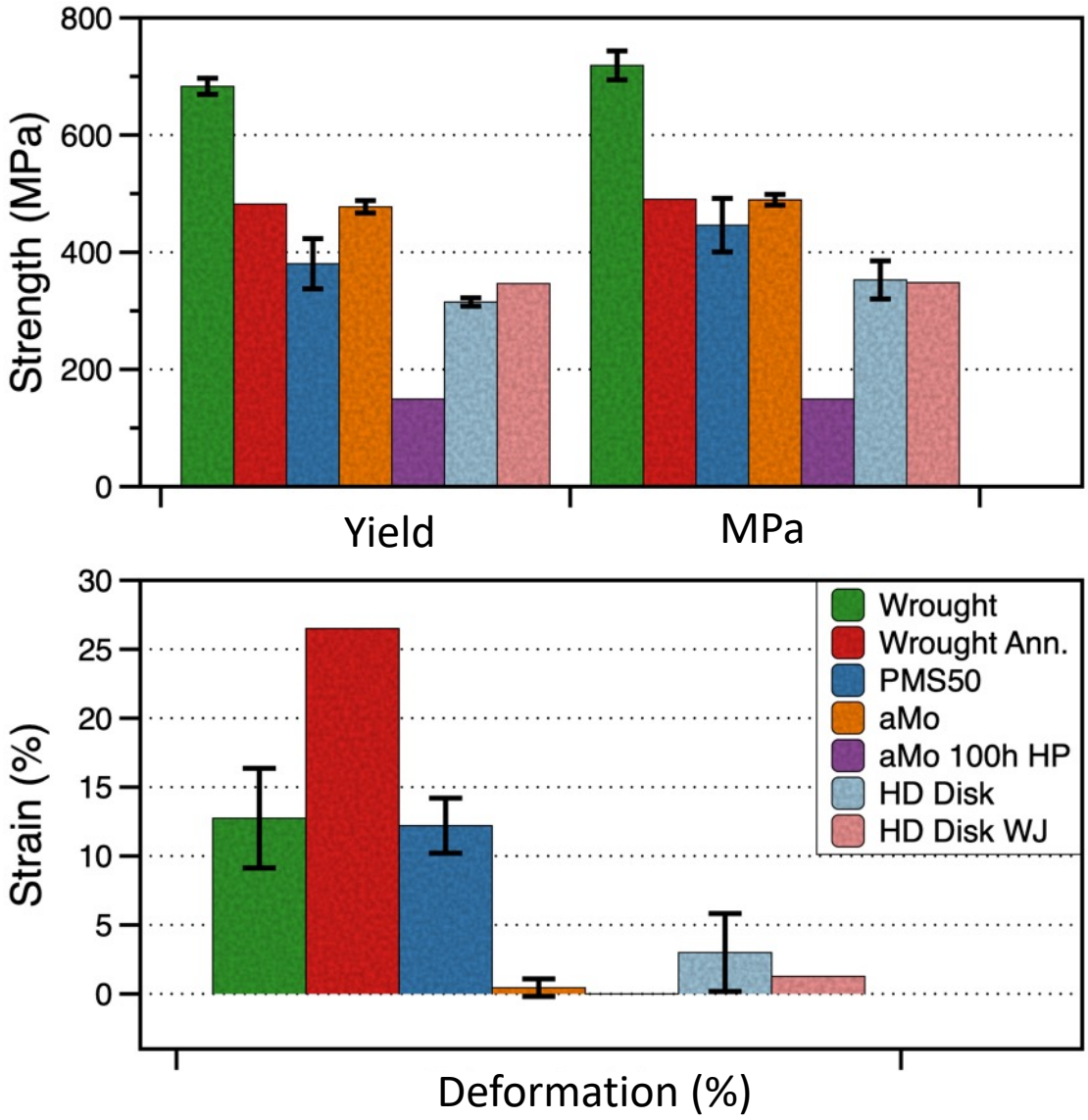

Figure 13: Comparison of the tensile properties between wrought Mo sheet in the as-fabricated or vacuum annealed conditions, the as-fabricated PMS50 Mo thin plates, the aMo disks in the as fabricated or annealed for 100 h in UHP He at 1000 °C conditions, and the HD Mo disks machined by EDM or water jetting (WJ).

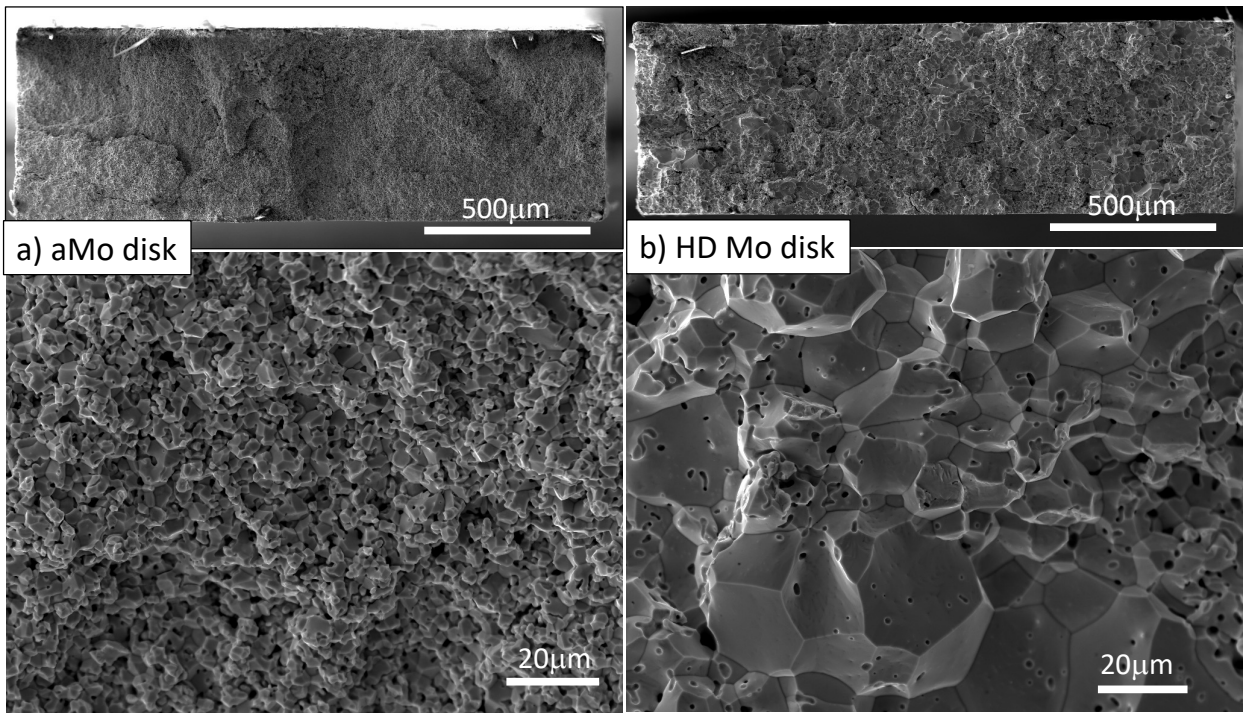

Figure 14: BSE-SEM images of the fracture surface after tensile testing at room temperature, a) aMo disk, b) HD Mo disk

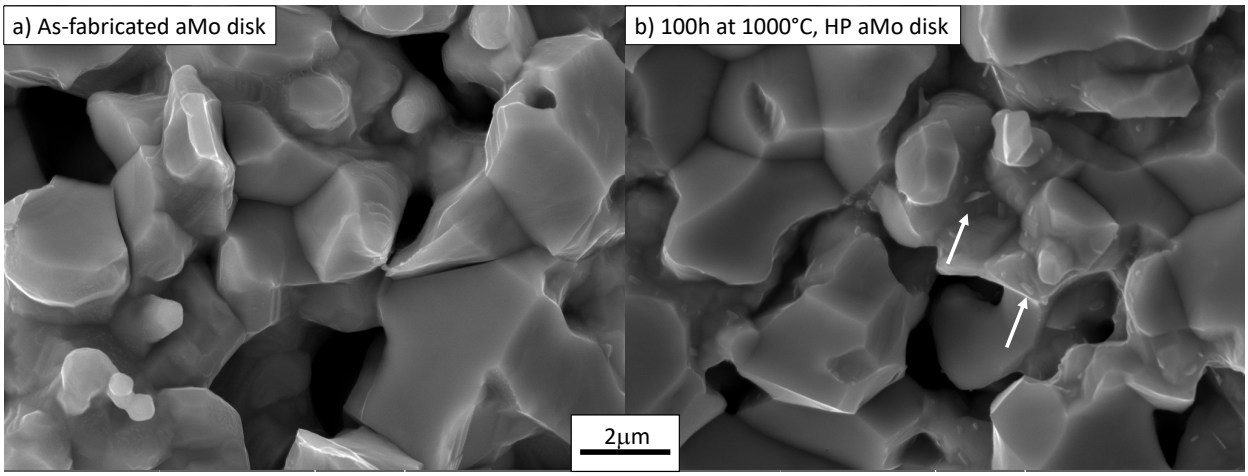

Figure 15: BSE-SEM images of the fracture surface of aMo specimens after tensile testing at room temperature, a) as fabricated, b) after exposure for 100 h in flowing HP He at 1000 °C

4. CONCLUSION

Tensile testing at room temperature was conducted on wrought 0.5 mm stress-relieved Mo plate, thin plates of PM Mo sintered at ORNL at 1600°C (PMS50) and aMo and HD Mo disks provided by NorthStar. The wrought Mo material showed an increase of ductility and decrease of yield strength and

UTS after annealing at 1000°C in vacuum due to partial material recrystallization. Exposure in flowing He with O2 content varying from ~1 to 15 ppm O_2 at 1000 °C resulted in a decrease of both alloy strength and ductility, the longer the exposure time, the lower the ductility. The material embrittlement was attributed to segregation of oxygen at grain boundary leading to brittle intergranular fracture, as proposed by Liu et al[2]. The PMS50 material exhibited a similar behavior but with a drastic decrease of strength and ductility after exposure at 1000 °C in flowing He with O_2 content <5ppm. The key differences were the embrittlement also observed for the specimen annealed in vacuum at 1000 °C, and the presence of small Mo oxide precipitate in the fracture surface. It is postulated that the oxygen trapped in the PM material can diffuse to grain boundaries during annealing at 1000 °C, leading to specimen embrittlement without the need for an exterior oxygen source.

Both the aMo and HD Mo disks exhibited very brittle tensile behavior at room temperature with several specimens failing after a plastic deformation of less than 1 %. This is likely related to the high density of voids present in both as fabricated disks, and the significant material inhomogeneity for the HD disks. Annealing of an aMo specimen in flowing high purity He led to a further embrittlement of the material, with again the presence of Mo oxides at the fracture surface confirming the role played by oxygen in grain boundary embrittlement. A higher material density and better control of the microstructure would be required to improve the Mo disk ductility and avoid in-service failures. Low levels of oxygen (<5ppm O_2) in flowing He were sufficient to embrittle wrought and PM Mo materials after exposure at 1000°C.

5. ACKNOWLEDGEMENTS

The authors would like to thank J. Wade, C. O'Dell, V. Cox, T. Lowe and K. Hedrick for their help with specimen preparation and microstructure characterization. They also would like to acknowledge H. Hyer and T. Muth for reviewing the manuscript. R. Lowden provided the PMS50 specimens. This research was sponsored by the U.S. Department of Energy's National Nuclear Security Administration (DOE/NNSA), Office of Material Management and Minimization, Molybdenum-99 Program.

6. REFERENCES

1. K.A. Woloshun, G.E. Dale, E.R. Olivas, F.P. Romero, D.A. Dalmas, S. Chemerisov, R. Gromov, R. Lowden, "Thermal Test on Target with Pressed Disks", United States, 10.2172/1245565 (2016).
2. S. Dryepondt, A. Willoughby, B. Johnston, "Oxidation of Molybdenum at 800°C and 1000°C in Flowing He with 0.5 to 250ppm O_2, ORNL report, ORNL/SPR-2022/2490 (2022).
3. C.T. Liu, S.H. Anderson, H. Inouye, " Effect of Oxidizing Environment on Mechanical Properties of Molybdenum and TZM.", ORNL-5431 (1978).
4. E. M. Passmore, "Correlation of Temperature and Grain Size Effects in the Ductile-Brittle Transition of Molybdenum", Philosophical Magazine, 8, 441-450 (1965).
5. B.V. Cockeram, R.W. Smith and L.L. Snead, "The influence of fast neutron irradiation and irradiation temperature on the tensile properties of wrought LCAC and TZM molybdenum", 346, 145-164 (2005).
6. S.C. Srivastava and L.L. Seigle, "Solubility and Thermodynamic Properties of Oxygen in Solid Molybdenum", Metallurgical Transaction, 5, 49-52 (1974).

7. K. Leitner, P.J. Felfer, D. Holec, J.Cairney, W. Knabl, A. Lorich, H. Clemens, S. Primig, “On grain boundary segregation in molybdenum materials”, Materials and Design 135, 204–212 (2017).
8. A. Kumar and B. L. Eyre, “Grain Boundary Segregation and Intergranular Fracture in Molybdenum”, Proceedings of the Royal Society of London. Series A, Mathematical and Physical Sciences, 370 , 431-458 (1980).
9. X.J. Yu and K.S. Kumar, “Uniaxial, load-controlled cyclic deformation of recrystallized molybdenum sheet”, Materials Science and Engineering A, 540, 187-197 (2012).
10. L. L. Snead, D. T. Hoelzer, M. Rieth and A.A.N. Nemith, “Refractory alloys, Vanadium, Niobium, Molybdenum, Tungsten, Structural Alloys for Nuclear Energy Applications,” Edited by G.R, Odette and S.J. Zinkle, 585-640 (2019).
11. B.V. Cockeram, E.K. Ohriner, T.S. Byun, M.K. Miller, L.L. Snead, “Weldable ductile molybdenum alloy development”, Journal of Nuclear Materials 382, 229–241 (2008).